

# COURSES

C1

## STRUKTURNÍ DATABÁZE ORGANICKÝCH A ORGANOMETALICKÝCH SLOUČENIN

Jindřich Hašek

*Institute of Macromolecular Chemistry, AS CR, Heyrovského nám.2, 162 06 Praha 6,  
hasek@imc.cas.cz*

### Introduction

**Strukturní databáze organických a organometalických struktur „Cambridge Structural Database (CSD)“** distribuovaná střediskem "Cambridge Crystallographic Data Centre (CCDC)" obsahuje v současné době okolo půl milionu publikovaných struktur organických a organometalických látek zjištěných experimentálně metodami difrakce rtg záření nebo difrakce neutronů. CCDC software umožňuje vyhledávání struktur, výpočet strukturních parametrů a statistickou analýzu strukturních rozdílů.

### Obsah databáze

CSD ve verzi "listopad 2008" obsahuje 457 000 organických a organometalických sloučenin. Přesnější definice sloučenin obsažených v databázi:

Sloučeniny obsahující alespoň jeden uhlíkový atom, a nepatří do následujících kategorií :

**Polypeptidy a polysacharidy** s více než 24 monomery. Tyto struktury jsou shromažďovány v "Proteinové strukturní databázi" na WWW adresách nebo <http://www.ebi.ac.uk/pdbe-site/PDBeSite/>

**Oligonukleotidy**, které jsou shromažďované v "Databázi nukleových kyselin" <http://ndbserver.rutgers.edu/>

**Anorganické struktury**, které jsou shromažďované v "Databázi anorganických krystalových struktur" [http://www.fiz-karlsruhe.de/icsd\\_contents.html](http://www.fiz-karlsruhe.de/icsd_contents.html)

**Kovy a slitiny**, které jsou shromažďované v "Databázi CRYSTMET®" na adrese <http://www.tothcanada.com/databases.htm>

### Software pro práci s daty uloženými v databázi CSD

**CONQUEST** – umožňuje vyhledávat struktury nejen podle chemického složení, sumárního vzorce ale výrazů použitých v textu, ale též podle uspořádání atomů či molekul v prostoru.

**PREQUEST** – umožňuje uživateli přidat do CSD databáze svoje vlastní (dosud nepublikované) struktury a provádět statistické analýzy s kompletní databází.

**MERCURY** – Velmi praktický a snadno ovladatelný program pro zobrazování a grafickou analýzu stavby krystalu a pro analýzu molekulární struktury

**VISTA** – Program pro statistickou analýzu dat získaných z CSD. Specializovaný tabulkový procesor s možností vhodné úpravy a analýzy získaných dat, tisk grafů, histogramů, atd. Data lze také exportovat do XLS formátu a pracovat v jiných tabulkových a grafických programech.

### Nadstavbové programy využívající znalosti získaných předchozí analýzou databázi

**MOGUL** – Program, který zobrazí statistiku požadovaných vazebných délek, úhlů nebo torzních úhlů pro zadaný strukturní fragment pro všechny struktury ve kterých byl tento fragment nalezený. Struktury odpovídající jednotlivým bodům jediným kliknutím zobrazíte a tak můžete snadno odfiltrovat nevhodné případy.

**ISOSTAR** – A collection of statistical analyses of intermolecular interactions containing 25022 scatterplots and 1550 theoretical studies derived from X-ray and NMR determined structures of 257162 organic and organometallic compounds and 7021 protein-ligand complexes. It describes combinations of 350 central function groups and 45 contact groups. User can view three dimensional distribution of frequency occurrence of intermolecular contacts (so called density surfaces). User has a possibility to add his own structures and prepare his own statistical analysis locally.

**SUPERSTAR** – program pro identifikaci interakčních míst in proteinech. Trojrozměrné mapy propensity zvýrazňují vhodná místa pro interakce vybraného proteinu s ligandy (vazebná místa proteinů).

**RELIBASE** – Program usnadňující analýzu struktury proteinů. Obsahuje databázi mezimolekulárních interakcí vytvořenou z dat obsažených v "Proteinové strukturní databázi" obsahující v současné době ~ 50 000 makromolekulárních struktur určených difrakcí rtg záření určených zpravidla pomocí rtg difrakce. RELIBASE obsahuje přehledy vazebných míst pro ligandy (substráty, inhibitory), které byly v komplexu experimentálně nalezeny rtg difrakcí a NMR, nebo které byly do experimentálně určené struktury proteinu namodelovány.

**HERMES** – Program pro grafické znázornění a analýzu interakcí mezi proteiny a ligandy (program Merkury pro proteiny nelze použít). Upraven zejména pro práci se systémy SuperStar, Relibase, GOLD, Mogul a IsoStar.



**GOLD** (Genetic Optimization for flexible Ligand Docking) - program nalezení optimálního umístění ligandu v molekule proteinu na základě pseudopotenciálů nastavených tak, aby vypočítané modely souhlasily co nejlépe s experimentálně stanovenými strukturami v CSD. Formálně jsou použity atomové a vazebné typy známé z programu SYBYL, ale empirické potenciály (force fields) a geometrická omezení (constraints), jsou odlišná. Program je tedy optimalizován tak, aby dával střední geometrii obdobných fragmentů pozorovaných v Cambridgeské [1] a Proteinové strukturní databázi [2]. Program vyžaduje kontrolu strukturních typů a pečlivé doplnění vodíkových atomů, ale počáteční poloha, orientace ligandů ani konformace bočních řetězců nejsou podstatné. Program používá "genetický algoritmus" pro hledání optimální cesty pro "zagarázování" ligandu v proteinu. Pracuje i s těžkými atomy. Statistické vyhodnocení výsledků garázování ligandu pro 83 komplexů protein-ligand dalo odhad chyby (RMSD) ~2.0 Å pro 81 procent případů.

**GoldMine** – Program pro usnadnění zpracování výsledků získaných programem GOLD při hledání optimálního zaparkování (docking) skupiny ligandů v proteinu a pro vyhodnocování optimálního ligandu pro různé váhy jednotlivých pseudopotenciálů vystupujících v účelové funkci (evaluation of ligands docking into proteins using different scoring functions).

**DASH** – Software pro řešení krystalových struktur z práškových dat, tj. na základě měření práškových difraktogramů. Program využívá metodu "simulated annealing" k hledání globálního minima účelové funkce.

C2

## WORKSHOP ON JANA2006

Michal Dušek and Václav Petříček

*Institute of Physics of the ASCR, v.v.i., Na Slovance 2, 18221 Praha, Czech Republic*

Jana2006 [1] is the last generation of the computing system Jana. Its development has started in early eighties when Václav Petříček developed several programs for analysis of three-dimensional structures from single-crystal X-ray diffraction data known as the SDS system. Later on, during the stay in Buffalo, USA, he wrote program Jana specialized to refinement and Fourier calculations for modulated structures. Both systems were developing separately until 1998 when they have been merged into a universal system Jana98. Another important milestone was adding a support for powder refinement in 2001 and possibility of an arbitrary combination of data sources in 2006. The latest development aims to magnetic structures, electron diffraction and, at the same time, to user friendliness. Jana system has currently about 1300 registered users around the world and it is almost exclusive tool for solution of modulated and composite structures.

Cambridgeská strukturní databáze je provozována obvykle jako lokální instalace pod systémem MS Windows licencovaná pro jednu IP adresu (objednávky na adrese: hasek@imc.cas.cz). Internetový přístup je možný pouze po registraci ve Fyzikálním ústavu AV ČR (kontakt: dusek@fzu.cz).

Licence na používání Cambridgeské strukturní databáze je placena jednou ročně. Nový software a data jsou dodávány v jarních měsících na DVD a nově přibývající data je možné doplňovat stahováním doplňků ze serveru <http://www.ccdc.cam.ac.uk>. Licence pro české uživatele se vztahují pouze na nekomerční uživatele [3].

Nadstavbové programy GOLD, DASH, RELIBASE+ a SUPERSTAR jsou distribuovány přímo administrativním centrem v Cambridge [http://www.ccdc.cam.ac.uk/contact/obtaining\\_products/](http://www.ccdc.cam.ac.uk/contact/obtaining_products/) pouze jako lokální licence. Od všech produktů je možné vyžádat si "free evaluation copy".

Příklady aplikací Cambridgeské strukturní databáze v různých vědních oborech lze nalézt například v níže uvedené literatuře [1, 2, 3, 4].

### LITERATURA

1. J. van de Streek, *Acta Cryst.*, **B62**, (2006), 567-579.
2. A. G. Orpen, *Acta Cryst.*, **B58**, (2002), 398-406. Applications of the Cambridge Structural Database to molecular inorganic chemistry.
3. F.H.Allen and W.D.S.Motherwell, *Acta Cryst.*, **B58**, (2002), 407-422. Applications of the Cambridge Structural Database in organic and crystal chemistry.
4. R. Taylor, *Acta Cryst.*, **D58**, (2002), 879-888. Life Science applications of the Cambridge Structural Database

The scope of Jana2006 is broad, from semi-automated service crystallography to difficult modulated structures. The user tools are universal; using Jana2006 for standard structures is therefore an advantage for anybody going to switch to modulated or difficult structures. In the field of **basic crystallography** the program offers usual tasks like automatic determination of space group, searching for higher symmetry, calling of SIR or Superflip [2] for structure solution, evaluation of Fourier maps, adding of hydrogen atoms etc. **Advanced tools** can be used for transformations, calculation of generally oriented Fourier sections, definition of twinning or rigid bodies, multiphase refinement, multipole refinement, introduction of local symmetry etc. We should point our elaborated transformation tools enabling seamless group-subgroup transformations necessary for investigation of merohedric twinning. The rigid body approach is very important for description of disorder of organic molecules and for lowering number

of refinement parameters when the structure model gets complicated. Another powerful concept are user equations, restraints and constraints which can define arbitrary linear relationship between the parameters of the structure model.

**Incommensurate structures** can be investigated up to the dimension 3+3. The superspace symmetry can be found from the diffraction pattern using the same semi-automatic tools like for standard structures. Jana2006 offers traditional harmonic modulation functions for occupancy, position and ADP as well as discontinuous functions (crenel and sawtooth). In the crenel-like description the positions and ADP parameters can also be described with Legendre polynomials. Rigid bodies can also be modulated. The modulated structures can be visualized by calling an external plotting program for a structure transformed to P1 symmetry, by plotting modulated parameters as function of  $t$  coordinate or by investigating two-dimensional sections by 3+d-dimensional Fourier map. For solution of modulated structures Jana2006 can directly call program Superflip based on charge flipping which can also be used for verification of superspace symmetry. **Commensurate structures** represent very useful concept for description of structure families. Jana2006 can determine a supercell symmetry corresponding to the  $t$  value used for the calculation and it can transform commensurate structure for a given  $t$  to the equivalent three-dimensional supercell. **Composite (or intergrown) structures** are also supported.

C3

## REAL STRUCTURE OF POLYCRYSTALLINE MATERIALS

### Short course

R. Kužel

Faculty of Mathematics and Physics, Charles University in Prague, Ke Karlovu 5, 121 16 Prague 2  
kuzel@karlov.mff.cuni.cz

#### 1. Introduction

During last decades, it has been shown many times that properties of materials are not determined only by phase composition and crystal structure but very often the so-called real structure plays an important role. What should we imagine under this name – *real structure of polycrystalline materials*? There is no clear definition but in the most general view it is any violation of ideal translation periodicity of atoms. If we consider a single crystal, this is already its finite dimension, the *surface* that breaks the periodicity and may lead to creation of a new 2D structure. This is not usually understood as real structure, though, but rather it belongs to a large and important branch of science – surface crystallography, surface physics and surface chemistry (see also [1, 2]).

Other deviations from ideal atomic positions are *thermal lattice vibrations*. They can be studied by several methods, in particular, by neutron scattering and they are considered in XRD in terms of the so-called Debye-Waller factors. The factors are sometimes approximated by a mean isotropic DW factor common for all atoms but exactly they

Jana2006 can combine powder and single crystal diffraction data from X-ray, synchrotron and neutron diffraction. The most practical issue is combination of powder neutron data with single crystal synchrotron or X-ray data measured at similar conditions, which is useful for differentiation of chemical elements in mixed sites or reliable determination of hydrogen positions. Another possibility concerns the latest option just being developed in Jana2006: it is possible to combine refinement of magnetic structure from powder data with nuclear structure from synchrotron data. The latest version of Jana2006 contains a convertor between representation analysis and magnetic (super)space groups which enables crystallographic approach to magnetic structures.

A workshop on all topics covered by Jana2006 would last many days. Because in the Czech Republic Jana software is rather rarely used the main focus of the present workshop will be on standard three-dimensional structures. Using single crystal and powder diffraction data of a simple structure we shall present the basic “philosophy” of the program. The rest of the workshop will deal with moderately difficult problems like twinning, mixed-sites refinement and disorder. Finally, solution of a simple modulated structure will be presented.

1. [www-xray.fzu.cz/jana](http://www-xray.fzu.cz/jana)
2. [superspace.epfl.ch/superflip](http://superspace.epfl.ch/superflip)

should be included in the product with individual atomic scattering factors and even better in anisotropic form and perhaps also including anharmonic contributions. However, the vibrations are not meant under the name “real structure” either.

For **single crystal**, the term is closely connected to the lattice defects. There are many types of lattice defects – point, line, plane (2D) or volume (3D). Some of them are schematically shown in Fig. 1. There are several methods for study of point defects like differential thermal expansion, positron annihilation (e.g. [3]), resistivity, specific heat and, of course, also imaging methods with high resolution like HRTEM, STM, AFM, FIM. The line defects – dislocations and higher dimension defects can be traditionally studied by TEM. In the framework of kinematical theory of diffraction the lattice defects can be divided into two kinds according to their influence on the diffraction pattern. This has been derived and suggested by Krivoglaz [4]. The lattice defects of the first kind are the defects with rapidly decreasing field and lead to the reduction of integrated intensity (static Debye-Waller factor), shift of the Bragg peaks and appearance of diffuse scattering. The defects of

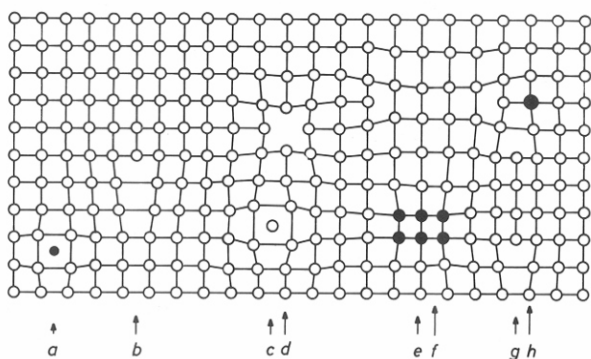


**Figure 1.** Picture of different types of lattice defects - a) Interstitial impurity atom, b) Edge dislocation, c) Self interstitial atom, d) Vacancy, e) Precipitate of impurity atoms, f) Vacancy type dislocation loop, g) Interstitial type dislocation loop, h) Substitutional impurity atom ([3])

the second kind with slowly decreasing ( $1/r$ ) displacement field, destroy the Bragg sharp peak and only concentrated diffuse scattering can be observed as the broadened quasiline – the lattice defects of the second kind. Point defects, their clusters, precipitates and small dislocation loops belong to the former while dislocations to the latter type. The type of displacement field plays the most decisive role for the classification of the defects. This is based on the physical nature of the defects and it has been derived for their random distribution. However, the situation is more complicated in practice. Only a few models for non-random defect distribution have been developed and used so far.

Since different effects are produced by both lattice defect types, different X-ray methods are applied for their investigation. The studies of defects of the first kind are mostly restricted to single crystals and consist in simultaneous measurement of lattice parameters, static Debye-Waller factors and whole maps of *diffuse scattering*. The diffuse scattering is probably the best source of information on point defects and their clusters since it is very sensitive to the type, arrangement and orientation of the defects and often even a simple comparison of experimental and simulated contour plots can be very helpful. The study of defects of the second kind can also be done for polycrystalline samples and it consists in the *XRD line profile analysis*. The classification of the lattice defects from the point of view of XRD should not be mixed with the classification of stresses. In this connection, all the distortions by point and line defects belong to the so-called 3<sup>rd</sup> kind stresses.

In addition to the above effects, **real structure of polycrystalline materials** includes also larger scale effects. This is distribution of size and orientation of individual grains and also their interactions, stresses (Fig. 2). The maps of grains are nowadays studied more and more by the EBSD (Electron backscattered diffraction) [5], very powerful method which however, is quite critical to sample preparation. 3D maps can also be constructed from XRD measurements of individual grains by synchrotron radiation [6, 7] (beamlines in APS and ESRF). In X-ray laboratory, such studies are always connected with measurements of diffracted intensities of individual ( $hkl$ ) planes in de-

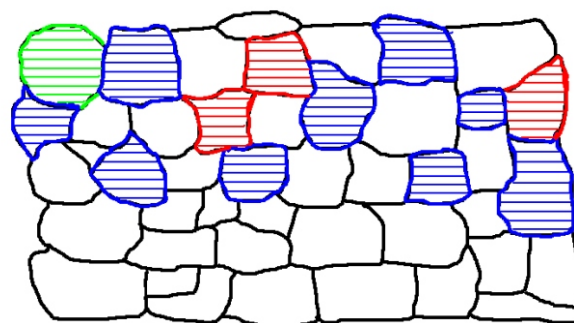


**Figure 2a.** Preferred grain orientation may cause significant changes of integrated intensities of  $hkl$  peaks in symmetric scans and their variation with inclination of corresponding planes with respect to the specimen surface.

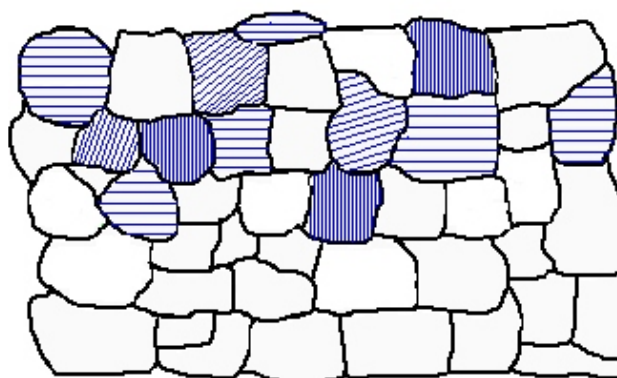


**Figure 2b.** Residual stress results in variation of interplanar spacing with inclination of the planes with respect to the specimen surface.

pendence on the orientation of the plane with respect to the specimen coordinate system – for texture investigation and/or diffraction peak positions (lattice spacing) in the same dependence – for residual stress measurement.

The investigation of real structure by diffraction methods is of great interest nowadays and still many unresolved problems. Several books appeared on the topics [e.g. 8, 9].

## 2. XRD line profile analysis

XRD line profile analysis is used for the determination of microstrain and/or dislocation density, crystallite size and sometimes also other defects like stacking faults. All these factors cause XRD line broadening. There are number of ways how they are included in present Rietveld programs. In most cases, though, phenomenological models are used and their main aim is to correct the pattern for these defects in order to refine crystal structure or make phase analysis and no to determine the above parameters.

### 2.1 Characterization of individual profiles

The diffraction line profile can be expressed as the dependence of intensity (e.g. in cps – counts per second) on the diffraction angle  $2\theta$  or on the diffraction vector magnitude ( $s = 2 \sin \theta / \lambda$ ). The profile can be characterized by several

parameters related directly to some structural and/or microstructural parameters:

**peak positions** lattice parameters, lattice geometry, lattice defects, residual stress

**integrated intensities** atomic structure, texture, lattice vibrations

**peak widths** internal strains, coherent domain size, lattice defects

**peak shape** distribution of lattice defects and domains

Any of these characteristics can be determined from a single powder diffraction pattern for each phase separately. For the analysis of line broadening several parameters can be used:

**FWHM** (half-width, full width at half of peak maximum)  
Integral breadth ( ) – integrated intensity  $I$  over peak height in the finite range  $s_1$  to  $s_2$

$$\frac{\int_{s_1}^{s_2} I(s) ds}{I_{\max}} \quad (1)$$

The ratio of this two widths is sensitive to profile shape.

#### Moments

$$M^n = \int_{s_1}^{s_2} I(s)(s - s_0)^n ds \quad (2)$$

#### Fourier coefficients $C(n)$

$$I(s) = \sum_n C(n) \exp(2\pi i n d_{hkl}(s - s_0))$$

$$C(L) = \frac{1}{s} \int_{s_1}^{s_2} I(s) \exp[2\pi i L(s - s_0)] ds \quad (3)$$

$s = s_2 - s_1$  is the integration range,  $L$  is a variable in the direct space )

These parameters can be determined by about three different methods:

Direct analysis of isolated lines

Fitting of suitable analytic functions (Pearson, pseudo-Voigt, Voigt) to the groups of diffraction profiles

Total pattern fitting either with or without structural constraints

The first method can include background separation, smoothing,  $K_2$  elimination and determination of the above parameters. This was applied already in classical profile analysis [10, 11]. The  $K_2$  elimination was based mainly on Rachinger algorithm [12], in improved way for example in [13]. Different analytical functions were applied (comparison in [14, 15], other functions can be found in [16, 17]) for the second and/or third method.

## 2.2 Instrumental broadening

Unfortunately, similarly to other physical methods we cannot measure pure physical effect (broadening) but this is smeared out by the instrument. This can be described as mathematical convolution. Measured profile is usually denoted as  $h$ , instrumental as  $g$  and physical as  $f$ . Then  $h = f * g$

(or  $h(x) = \int f(y)g(x - y)dy$ ) and  $f$  profile must be obtained

by the deconvolution. There are a number of deconvolution methods but always with a problem of mathematically incorrect procedure since the functions are not known in infinite range and there is also experimental noise in the data [18]. The problems can be reduced by the so-called regularization but always there should be an effort to minimize instrumental broadening, i.e. to increase resolution. Of course, it goes always on the cost of intensity. If we can reduce the influence of  $g$ , then depending on a problem (ratio of physical to the instrumental broadening) the instrumental broadening can either be completely neglected or on the other hand finer physical effects can be measured (larger crystallites, lower defect densities). Conventional powder diffraction (parafocusing Bragg-Brentano) can have quite good resolution, in particular, if the primary  $\theta$  monochromator is used. The problem is in the analysis of thin films when the symmetric scan is often inconvenient because of larger penetration depth and for asymmetric scans parallel beam geometry is preferred (mirrors, parallel plate collimators). Depending on the used parallel plate collimator, this arrangement has usually rather poor resolution (about three times worse than Bragg-Brentano). The resolution can be improved by different ways - for example double-mirror setup, channel-cut monochromator, hybrid monochromator, crystal analyzers etc. but with sometimes drastically reduced intensity not very usable with conventional X-ray sources. The methods of deconvolution can be divided into several groups according to characterization of profiles – full profile deconvolution, Stokes correction of Fourier transform (Fourier transform of the convolution is a product of Fourier transforms), approximate methods of integral breadths (Voigt function) or simple subtraction of the second moments (variances). Another problem can be the determination of  $g$  profile. In most cases, standard sample with negligible physical broadening is measured under the same conditions as the investigated sample. NIST was selling LaB<sub>6</sub> standard for line broadening but this is out of stock now. Optimal standard should be the same material as the one investigated mainly because of absorption. This may be achieved by annealing of suitable sample but the results are uncertain. Therefore each laboratory should select suitable standards according to its experience. The second way may be to calculate  $g$  from known geometrical parts of the instrument (slits) and spectral lines. This has been suggested by R. W. Cheary [19] and it is used in commercial software TOPAZ (Bruker). The software uses also another popular way – to replace ill-defined deconvolution by the fitting of the pattern with a convolution of the known instrumental profile and physical or phenomenological function of several refineable parameters.

## 2.3 Physical broadening

Two components of line broadening are usually considered – size broadening, the component that is reflection order-independent (independent on the diffraction vector magnitude) and strain broadening proportional to the diffraction vector magnitude, increasing with the distance from the reciprocal lattice origin. The particle size effect is caused by interfaces (small crystal size, subboundaries,



stacking faults, twin boundaries) and the strain broadening can be connected to dislocation arrangement with a weak defect correlation that is determined by the mean total dislocation density and the mean outer cut-off radius of the strain field of dislocations. Internal stresses of the 2<sup>nd</sup> kind being constant within individual grains can be another reason for strain broadening. It can be characterized by the mean square strain. In next sections, the main attention will be devoted to the influence of the lattice defects. A short review of the methods was published in [20] and a review of dislocation line broadening appeared in [21] with many references.

### 2.3.1 Simple integral breadth methods, Williamson-Hall plot

Line broadening is often characterized by the so-called Williamson - Hall (WH) plot, i.e. dependence of integral breadth on  $\sin^2 \theta$ . This plot is based on the assumption of Lorentzian distribution of both domain size and microstrain, which means that both components (widths) are additive. This assumption is not very realistic though. The common relation can be generalized in the following form (breadths are in reciprocal space units  $1/d$ ),

$$\frac{K}{D_{hkl}} + 4e_{hkl} \frac{\sin^2 \theta}{\lambda} \quad (4)$$

which can be derived for several approximations of distributions for both components. The constants  $K$ ,  $e$ ,  $g$  depend on the considered analytical approximation of crystallite size and microstrain distributions. Both crystallite size  $D$  and microstrain  $e$  can be  $hkl$  dependent. Therefore the WH plot should be applied for more orders of selected reflection. However, it may also well be used in order to get an overall picture and first estimation of the weight of both size and strain components. It may be dangerous for quantitative analysis unless one of the components is significantly dominant (then it can be determined quite precisely). However, it is useful when the changes of both effects or their relations to the parameters of sample preparation are of main interest (e.g. deposition of thin films – temperature, substrate bias, deposition rate).

The size broadening (order-independent) term e.g. can be written as follows:

$$D_{hkl} = K_s^{hkl} V^{1/3} \quad (5)$$

where  $D_{hkl}$  is the so-called apparent crystallite size,  $V$  is the true size and  $K$  is the Scherrer constant. The constant is  $hkl$  dependent. The corresponding line broadening anisotropy is given by the anisotropic shapes of crystallites. The size term can also be related to stacking faults, microtwins and sharp dislocation walls. These defects can give specific  $hkl$  dependence too.

The strain (order-dependent) term for randomly distributed lattice defects can be written as follows

$$(1/d) = f(hkl) D_0 f(hkl) \frac{\sin^2 \theta}{\lambda} \quad (6)$$

where  $f$  is the function of the orientation factor,  $D_0$  depends on the defect strength and  $f$  is a function of the defect density. The  $hkl$ -dependence is given by the orientation factor. However, the strain terms can also include the so-called 2<sup>nd</sup> kind stresses which complicate the evaluation.

For dislocations the approximate formula given in [26] can be applied

$$\frac{1}{d} = \sqrt{\frac{f(hkl)}{M}} \frac{\sin^2 \theta}{\lambda} \quad (7)$$

where,  $b$  is the size of the Burgers vector of assumed dislocations,  $\lambda$  is the wavelength,  $\theta$  the diffraction angle.  $f_{hkl}$  is the so-called orientation or contrast factor determining the line-broadening anisotropy. It depends on the particular slip system, the dislocation character, the elastic anisotropy and the orientation of the diffraction vector with respect to the Burgers vector and the dislocation line. The main limitation of the method is the uncertainty of the correlation parameter of dislocation arrangement which is related to the line profile shape. This value is often written as  $M = r_c / \lambda$ , where  $r_c$  denotes the outer cut-off radius of dislocation strain field and  $\lambda$  is the dislocation density. Analytic approximation of the  $f(M)$  function is given in [26] as follows

$$f(M) = a \ln(M+1) + b \ln^2(M+1) + c \ln^3(M+1) + d \ln^4(M+1), \quad (8)$$

with  $a = -0.173$ ,  $b = 7.797$ ,  $c = -4.818$  and  $d = 0.911$

The  $M$ -factor can be estimated from the line shape for example in terms of the Voigt function approximation (the ratio of long-tail Lorentzian component of breadth to the short-tail Gaussian one,  $y = \int_{-\infty}^{\infty} g(x) dx$ ). Based on the data shown in [26], one can use an approximate relation  $M = 1/y$ . More precisely, the data can be fitted with the formula  $M = 0.96/y^{0.95}$ . The formula should be applied after the correction of the instrumental broadening by the method of the Voigt function which gives corrected values of  $r_c$ ,  $g$ . Even though the factors vary with  $hkl$  indices, a mean value of the  $M$ -factor averaged over all reflections was always used. The reason was that the individual factors obtained by the above procedure are influenced significantly by experimental (statistical) errors since each factor depends on four experimental values and their ratios (Gauss and Cauchy components of both instrumental and experimental profiles), and consequently may introduce more noise in otherwise quite stable experimental values of integral breadths. The method is very useful for estimation XRD line broadening anisotropy which sometimes can be used for the determination of dislocation types, in case of strain broadening or to determination of anisotropic crystallite size in case of dominant size broadening.

### 2.3.2 Fourier methods

The Fourier methods were connected from the beginning with the so-called Warren-Averbach analysis [27]. This is based on phenomenological model of mosaic blocks with

microstrains. In derivation of Fourier coefficients, the crystal is divided into columns of lattice cells which may be shifted due to strains and they are summed up in the diffraction formula. This summation, of course, depends also on the size of coherently diffracted domain – crystallites. Total Fourier coefficients are then products of size and strain terms. Under the assumption of not too large distortions and/or their Gaussian distribution, the procedure consists in plotting of logarithms of the Fourier coefficients on reflection order or  $1/d$ . These plots are linear in the first approximation with the intercepts giving the size Fourier coefficients and slopes the mean square microstrain. In final step, the size coefficients are plotted against the number  $n$  or real distance  $L$  ( $L = nd_1$ ,  $d_1$  is the interplanar spacing corresponding to the first order reflection). The initial slope give mean value of *crystallite size*. The other result is dependence of *microstrain* on the distance which may not be a constant.

For *microscopic models*, the strain Fourier coefficients can also be calculated. For example for not too correlated dislocations, the Fourier coefficients can be written as

$$\ln A_h(L) = B_h L^2 \ln \frac{r_c}{L} + B_h \sum_{i=1}^N b_i^2 \sin^2 \frac{2\pi h x_i}{L}, \quad (9)$$

where  $h$  denotes  $hkl$ ,  $i$  numbers  $N$  different slip systems and  $r_c$  is the so-called cut-off radius closely related to the correlation in dislocation arrangement. Then the evaluation of dislocation density can be done simply from the plot of  $\ln A(L)/L^2$  vs  $\ln L$ . However, real data does not follow exactly this dependence because relation (9) does not describe full profile so that one must take only medium linear range which is not always easy to select.

## 2.4 Multiple peak and total pattern fitting

The idea to replace several-steps of complete Fourier analysis including deconvolutions (instrumental profile, size-strain separation) by the single-step profile fitting of several reflection orders simultaneously and to replace deconvolution by convolution of the modeled physical and known instrumental profiles was first introduced by Houska [28, 29] in terms of classical phenomenological model and two size and two strain parameters. Nowadays, two program systems for multiple peak or total pattern fitting based on description by realistic microstructural model are being developed in groups of Paolo Scardi [e.g. 30-33, Pm2k by Matteo Leoni] and Tamas Ungar [34, MWPFIT by G. Ribárik]. Both are under development and latest versions also include stacking faults. The parameters fitted are usually – *mean crystallite size, variance of crystallite size distribution, dislocation density, dislocation correlation parameter*, sometimes also, *fractions of different dislocations, the densities of stacking faults*. A general problem for the whole pattern fitting is a high correlation between the dislocation density and dislocation correlation parameter ( $M$  or  $R_c$ ). The correlation is intrinsic in the description and cannot be completely overcome by using different optimization procedures. Actually, the correlation parameter influences mainly the profile shape (tails) but it is not very

sensitive to it and consequently the minimalization procedure cannot be sensitive enough to it either. In any case, high-quality data are required for successful fitting.

## 3. Preferred grain orientation – texture, residual stress

### 3.1 Effects in conventional symmetric $\theta$ - $2\theta$ scan

In case of non-random grain orientation individual integrated intensities of  $hkl$  peaks  $I_{hkl}$  may differ significantly from the values given primarily by the structure factors, the theoretical intensities  $R_{hkl}$ . The effect is usually corrected by some of more or less empirical corrections or the corrections obtained by simple models (e.g. March-Dollase). The corrections are included in all Rietveld type programs. Preferred orientation can be simply characterized by the so-called Harris texture indices  $T_{hkl}$  given by normalized ratios  $I_{hkl}/R_{hkl}$  that are equal to unity in case of random orientation. However, not always unexpected variations of intensities can be related to the texture. They may be connected to crystal structure itself or to poor grain statistics. In order to discover texture effects unambiguously, other than symmetrical scans must be used. The effects are usually not too strong for powders except those consisting of highly anisotropic particles but they may be huge for bulk materials and in particular thin films.

Residual stresses (1<sup>st</sup> kind stresses that are homogenous in larger volume over several grains) cause peak shifts and therefore change of lattice parameters. However, it may be difficult to ascribe the observed changes of lattice parameters directly to stresses since they can be caused also by some lattice defects and especially by chemical composition (e.g. stoichiometry). These stresses cannot exist in fine powders but similarly to textures, they may be rather high in bulk materials and thin films. Corrections are not included in most of Rietveld programs except Maud by Luca Lutteroti [35].

### 3.2 Asymmetric $\theta$ - $2\theta$ scans

For complete characterization of textures and stresses inclinations of specimen from symmetrical position are required. Some experiments can be performed on standard goniometers rotating the specimen around the goniometer axis ( $\omega$ ) but usually rotations around perpendicular axis ( $\psi$  or  $\chi$ ) are preferred. This can be realized by the Eulerian cradle. In order to reduce instrumental aberrations and increase intensity, parallel beam optics with polycapillary is preferred. Of course, the arrangement has low resolution.

Different characterization of texture can be realized.

*Texture indices* from conventional symmetric scan (see above)

*$\omega$ -scan or  $\psi$ -scan*. Very fast characterization. The detector is fixed in the Bragg position of measured diffraction peak  $hkl$ . The scan is performed by rotation of the specimen about the goniometer axis (or perpendicular axis, respectively). For random grain orientation the intensity is nearly constant, strong texture results in sharp peak. FWHM of the peak can be taken as a characterization of the texture degree. Any shift of the peak maximum from the original position (symmetric Bragg case) indicates inclination of the texture.



-scan. The detector is fixed in the Bragg position of measured diffraction peak. Rotation of the specimen around the surface normal. It must be done in asymmetric position (sample inclination) Intensities usually plotted in polar coordinates. Symmetric figure indicates fiber (axially symmetric) texture. Then also the  $\omega$ -scans may be a good characterization of the texture.

*Pole figure measurement.* The detector is fixed in the Bragg position of measured diffraction peak. Measurement of intensities for different specimen inclinations ( $\theta$ ,  $\phi$ ). Intensities shown in stereographic projection. Full characterization of texture

*ODF – orientation distribution function calculation from several pole figures.* The function describes the so-called 3D texture and it is used as a weight function for calculation of different physical properties of whole polycrystalline material.

For the stress determination, variations of lattice spacing with the crystal lattice plane inclination to the specimen surface must be measured. The geometry is usually identical with that for texture measurements. However, there are several ways how to measure the dependence

*2 $\theta$ -scan.* The angle of incidence is constant and small. The detector scan then gives information connected to the lattice planes ( $hkl$ ), in particular lattice spacings, differently inclined with respect to the surface for different  $hkl$ . Parallel beam geometry is required. Elastic anisotropy of the material may cause scatter of values.

*-2 $\theta$  scan on the  $\omega$ -goniometer.* The specimen is tilted by  $\omega$  from the symmetrical Bragg position around the goniometer axis and peak positions for different  $hkl$  are measured by  $-2\theta$  scan. This can be done for several  $hkl$ . However, for low angle peaks the range of possible angles  $\omega$  is geometrically restricted significantly.

*-2 $\theta$  scan on the  $\psi$ -goniometer.* The specimen is tilted by  $\psi$  in the Eulerian cradle around the axis perpendicular to the goniometer axis and peak positions for different  $hkl$  are measured by  $-2\theta$  scan. This can be done for several  $hkl$ . There are no significant geometrical restrictions for  $\psi$ .

In case of simple uniaxial or biaxial residual stress, the lattice spacings are linearly proportional to  $\sin^2$  (well-know  $\sin^2$ -method). If the stress is general, tri-axial, the dependence is not linear and different for positive and negative  $\sigma$ . Then more measurements must be done also for different rotations  $\phi$  but finally whole strain tensor can be determined. Always, the lattice spacing are measured only by XRD and for calculation of stresses, the so-called X-ray elastic constants must be known or measured under known external field. The constants can be calculated by using different models of interactions between grains (Reuss, Voigt, Kröner, Hill, Vook-Witt etc.). The dependence can also be non-linear because of gradients and/or simultaneous presence of texture and residual stress. This is the most complicated case which has been simulated but direct methods of measurements have been suggested only for particular cases. It may require measurement of the reciprocal space maps. These and, of course, also the above dependences are measured nowadays with the aid of different position sensitive detectors which improve largely the speed of data collection.

## 2. Total pattern fitting

The method has become very popular in last years but it often requires appropriate microstructural model capable of correct description of real material for example the effect of line profile anisotropy. Total pattern fitting without structural constraints was used in [37-38]. Rietveld structural refinement [39] is now included in several programs like Fullprof, GSAS etc. (see [40]). It usually includes also phenomenological description of real structure by anisotropic microstrain and anisotropic crystallite size in terms of general ellipsoids. This approach may be very useful especially for appropriate corrections during structure refinement. For obtaining of the above parameters of real structure (see 2.3.3) the programs Pm2k or MWPFIT are recommended

Program MAUD [35] is nowadays probably the best for the Rietveld type evaluation of textured and stressed samples, for example thin films but does not include dislocation models and stacking faults. Z. Matěj is developing a program – expanded FOX [36] based on Crystal Objects library that includes some of the features of the above programs. It can apply easily structural constraints, includes dislocation models, stacking faults, simplified corrections for texture and also the residual stress. Most of these corrections are optional, i.e. the peak intensities and positions can be either constrained or refined independently. This is quite important feature since not always the correct descriptions of all effect are available. In case of very strong textures and stresses whole reciprocal space maps must be measured. Of course, their fitting is rather complicated but also possible [35, 41].

1. R. Kužel, *Materials Structure*, 14 (2007) 103.
2. J. Fiala, I. Kraus, *Materials Structure*, 16 (2009) this issue.
3. [http://www.tf.uni-kiel.de/matwis/amat/def\\_en/overview\\_main.html](http://www.tf.uni-kiel.de/matwis/amat/def_en/overview_main.html).
4. Krivoglaz, M. A.: X-ray and Neutron Diffraction in Nonideal Crystals. Springer-Verlag, Berlin, 1996.
5. M. Dopita, *Materials Structure*, 16 (2009) this issue.
6. H. F. Poulsen, S. F. Nielsen, E. M. Lauridsen, S. Schmidt, R. M. Suter, U. Lienert, L. Margulies, T. Lorentzen and D. Juul Jensen, *J. Appl. Cryst.* 34 (2001) 751-756.
7. B. Jakobsen, H. F. Poulsen, U. Lienert, W. Pantleon, *Acta Materialia*, 55 (2007) 3421-3430.
8. Defect and Microstructure Analysis by Diffraction. Ed. by R. L. Snyder, J. Fiala and H. J. Bunge, Oxford University Press, 1999, pp. 127-140.
9. Diffraction Analysis of the Microstructure of Materials, edited by E. J. Mittemeijer, P. Scardi, Springer, Berlin, Heidelberg, 2003.
10. H. P. Klug, L. E. Alexander, X-ray Diffraction Procedures for Polycrystalline and Amorphous Materials. New York, 1974.
11. C. N. J. Wagner, Program DIFFAN, Yale University Connecticut 1965.
12. W. A. Rachinger, *J. of Sci. Instruments* 25, 254, (1948).
13. J. Ladell, A. Zagofsky, S. Pearlman, *J. Appl. Cryst.* 8, 499-506 (1975).



14. S. A. Howard, R. L. Snyder, *Advances in X-ray Analysis*, 26, 73-80 (1983).
15. R. A. Young, D. B. Wiles, *J. Appl. Cryst.* 15, 430-438 (1982).
16. W. I. F. David, J. Mathewman, *J. Appl. Cryst.* 18, 461-466 (1985).
17. N. Pyrrros, C. R. Hubbard, *J. Appl. Cryst.* 16, 289-294 (1983).
18. M. Čerňanský, *Materials Structure*, 11 (2003) 72-74.
19. R. W. Cheary, A. Coelho, *J. Appl. Cryst.* 25 (1992) 109-121.
20. R. Kužel, *Materials Structure*, 11 (2003) 75-79.
21. R. Kužel, *Z. Kristallogr.*, 222 (2007) 136-149.
22. G.K. Williamson and W.H. Hall, *Acta Metall.* 1 (1953) 22-31.
23. R. Kužel, R. Černý, V. Valvoda, M. Blomberg and M. Merisalo, *Thin Solid Films* 247 (1994) 64-78.
24. J. I. Langford, D. Louer and P. Scardi, *J. Appl. Cryst.* 33 (1999) 964-974.
25. J. I. Langford and A.J.C. Wilson, *J. Appl. Cryst.* 11 (1978) 102.
26. E. Wu, A. MacGray, E. H. Kisi: *J. Appl. Cryst.*, 1998, vol. 31, pp. 356-362.
27. Warren, B. E.: *X-Ray Diffraction*. Addison-Wesley. Reading. 1969.
28. T. Adler, C. R. Houska, *J. Appl. Phys.* 17 (1979) 3282-3287.
29. C. R. Houska, T. M. Smith, *J. Appl. Phys.* 52(2) (1981) 748-754.
30. P. Scardi, M. Leoni, in *Diffraction Analysis of the Microstructure of Materials* (Eds. E. J. Mittemeijer, P. Scardi) pp.51-92. Springer. Berlin. Heidelberg. 2003.
31. P. Scardi, M. Leoni, *Acta Cryst. A* 58 (2002) 190-200.
32. P. Scardi, M. Leoni Y. H. Dong, *Eur. Phys. J.* B18 (2000) 23-30.
33. M. Leoni, T. Confente, P. Scardi, *Z. Kristallogr.*, Suppl. 23 (2006) 249-254.
34. G. Ribárik, T. Ungár, J. Gubicza, *J. Appl. Cryst.* 34 (2001) 669-676.
35. <http://www.ing.unitn.it/~maud/>.
36. Z. Matěj, L. Nichtová, R. Kužel, *Materials Structure*, 15 (2008) 46-49.
37. H. Toraya, *J. Appl. Cryst.* 18, 351-358 (1985).
38. H. Toraya, *J. Appl. Cryst.* 19, 440-447 (1986).
39. The Rietveld Method, ed. R. A. Young, IUCr series, Monographs on Crystallography (1995).
40. <http://www.ccp14.ac.uk/index.html>
41. D. Šimek, R. Kužel, D. Rafaja, *J. Appl. Cryst.* 39 (2006) 487-501.